NJC

Accepted Manuscript

This article can be cited before page numbers have been issued, to do this please use: J. H. Jeong, H. X. Ma, D. Y. Kim, C. W. Kim, I. H. Kim, J. W. Ahn, D. S. Kim and Y. S. Kang, *New J. Chem.*, 2016, DOI: 10.1039/C6NJ02436J.

View Article Online
DOI: 10.1039/C6NJ02436J

NJC

ARTICLE

Cite this: DOI: 10.1039/x0xx00000x

Chemical Synthesis of $Nd_2Fe_{14}B$ Hard Phase Magnetic Nanoparticles with Enhanced coervivity value; Effect of CaH_2 Amount on the Magnetic Properties

Received 00th January 2014,
Accepted 00th January 2014

DOI: 10.1039/x0xx00000x

www.rsc.org/

Ji Hun Jeong,[a] Hao Xuan Ma,[a] *Doyun Kim,*[a] Chang Woo Kim,[a] In Ho Kim,[a] Jae Woo Ahn,[a] Dong Soo Kim[b] and Young Soo Kang[a,*]

The $Nd_2Fe_{14}B$ hard phase magnetic nanoparticles were successfully synthesized by a chemical synthesis route followed by reduction and diffusion process without consuming a large amount of energy. $Nd(acac)_3{\cdot}xH_2O$, $Fe(acac)_3$ and $(C_2H_5)_3NBH_3$ were used as precursors and CaH_2 was used as a reducing agent for the reduction and diffusion process. The crystal structure and compositions of resultant Nd-Fe-B nanoparticles were detected with X-ray Diffraction (XRD) and energy dispersive X-ray spectrometer (EDX) measurements. The overall morphologies and magnetic properties of final products were measured with Transmission electron microscopy (TEM) and vibrating sample magnetometer (VSM) at 300 K. The detailed reductive effect of CaH_2 relative quantity on magnetic properties of final products was studied with the different mixing weight ratio of CaH_2 to the preliminary reduced metal oxide powders by checking with High resolution TEM (HRTEM), XRD and VSM measurements. The different mechanisms on the reduction and diffusion process with different amount of CaH_2 were comparatively studied. Deficient amount of CaH_2 resulted in the residual unreduced metal oxide powders, decreasing magnetic coercivity. On the other hand, excessive amount of CaH_2 evolved H_2 gas during washing process with water, bringing hydrogenation of $Nd_2Fe_{14}B$ to produce $Nd_2Fe_{14}BH_x$. The relative amount of CaH_2 had a critical effect on the magnetic properties of the prepared $Nd_2Fe_{14}B$-nanoparticles

Introduction

Rare earth (RE) transition metal permanent magnet offering high coercivity and energy product have drawn tremendous attention in the magnetic materials research field.[1,2] One of the most promising magnetic material is $Nd_2Fe_{14}B$ discovered by Sagawa *et al*.[2] Especially, the higher anisotropy field value of $Nd_2Fe_{14}B$ has given a promoted larger coercivity value, leading to high energy products. Thus, $Nd_2Fe_{14}B$ magnets have shown the highest maximum energy product (BH_{max}) with highly ferromagnetic performance and have been used in a wide range of applications such as generators, electric motors, electrical devices and magnetic separators, *etc*.[3,4,5]

Most of the research on the synthesis of the hard magnet, $Nd_2Fe_{14}B$, are focused on the powder metallurgy methods, rapid quenching techniques and the hot melt spinning process. These mechanical methods including ball milling and melt spinning have

a Department of Chemistry, Sogang University, Seoul 121-742, Republic of Korea. E-mail: yskang@sogang.ac.kr; Fax: +82 2701 0967; Tel: +82 2701 6379

b Korea Institute of Material Science, Changwon, Gyeongnam 642-831, Republic of Korea. E-mail: dskim@kims.re.kr

View Article Online
DOI: 10.1039/C6NJ02450D Journal Name

shown high magnetic properties of the maximum energy product in the range of 320 – 440 kJm^{-3} due to its increased packing density of the particle, resulting in the elongation of the single domain. However, they demands high energy consumption, and moreover, it is difficult to obtain the optimized ratio of the alloy composition and the size of the particles and its magnetic grains. These would be critical limitations for its practical application in the spin exchange coupling among the soft and hard permanent magnets, which has the great potential to acquire higher maximum energy product. Even though it is difficult, it is also possible to get a good performance of exchange coupled magnet with critical control of fabricating techniques.[6]

On the other hand, soft chemical route to synthesize magnetic nanoparticles controlling reduction and diffusion conditions and crystal orientation of nanoparticles has advantage in manipulating size of particles and magnetic grains, resulting in a high magnetic performance and usability to the spin exchange coupling of the soft and hard magnets.[7,8] However, the reduction potential of Nd^{3+}/Nd^0 is E^0 = -2.323 eV and it is much lower than that of the reduction of Fe^{2+} ion, E^0 = - 0.447 eV of Fe^{2+}/Fe^0. Also, the low chemical stability of Nd-Fe-B metal alloys in the ambient condition as well as the difficulty in removal of non-magnetic phases such as Ca and CaO after reduction process can be important problems in applying it in various scientific fields with relatively low maximum energy product.[9] These large difference of the reduction potential and the low chemical stability of Nd-Fe-B magnets make the co-reduction and synthesis be a challenging issue.

Even though the preparation of magnetic nanoparticles using soft chemical synthesis route is challenging, the method controlling the size of particles and grains is still a crucial synthesis technique for the further application on the fabrication of exchange coupled magnet which has a higher energy density.[10-13] For these reasons, the soft chemistry method to synthesize $Nd_2Fe_{14}B$ magnetic nanoparticles have drawn more attention because of easy fabrication for the nano-size composition of them, and it is convenient for the synthesis of exchange coupled magnet in the further work.[14-18]

Recently, Kang *et al*. have reported a nitrate-citrate auto-combustion method to prepare Nd-Fe-B metal alloys by the reduction and diffusion process with low energy consumption and get higher magnetic properties compared with the results of the previous reports.[19] They have also reported a facile synthesis method using sodium borohydride and the magnetic phase transformation of Nd-Fe-B nanoclusters by oxygen bridging.[20] Ramanujan *et al*. have reported a novel synthesis method of $Nd_2Fe_{14}B$ hard magnetic nanoparticles by microwave assisted combustion followed by the reduction process and sol-gel based chemical synthesis route.[21,22]

Herein, we report the chemical method for the synthesis of $Nd_2Fe_{14}B$ magnetic nanoparticles without consuming a large amount of energy comparing with traditional mechanical methods. This process should facilitate the synthesis otherwise it is difficult due to high negative reduction potential of neodymium. The method includes the conversion of metal acetyl acetonate precursors to metal oxide *via* heating operation relatively at low temperature. The solution was stirred vigorously for homogeneous dispersion and washed with ethanol and hexane for the metal oxide powders. After then, reductive annealing process was carried out with CaH_2 as a reducing agent at 800 - 900 °C under Ar gas atmosphere. From this experiment, $Nd_2Fe_{14}B$ magnetic nanoparticles were easily obtained. In additional study, the effect of CaH_2 quantity on magnetic properties of final products was also investigated with the different mixing weight ratio of the preliminary reduced metal oxide powders to CaH_2 with HRTEM image, XRD and VSM measurements.

Journal Name

View Article Online
DOI: 10.1039/C6NJ02436D ARTICLE

Experimental

Materials

$Fe(acac)_3$ (≥99.9%, Sigma Aldrich), $Nd(acac)_3{\cdot}xH_2O$ (Sigma Aldrich), $(C_2H_5)_3NBH_3$ (97%, Sigma Aldrich), oleylamine (70%, Sigma Aldrich), CaH_2 (95%, Sigma Aldrich), cyclohexane (anhydrous 99.5%, Sigma Aldrich) were used as obtained without further purification. Deionized water was purified by using Milli Q water purification system. All synthesis procedures were carried out under oxygen-free conditions using a standard Schlenk-line set-up.

Synthesis

Step 1: Synthesis of Nd-Fe-B oxide powders

The synthesis of $Nd_2Fe_{14}B$ magnetic nanoparticles was carried out by soft chemistry method. The flow diagram of the synthetic process is shown in Fig. 1. For the synthesis of Nd-Fe-B oxide powders, $Nd(acac)_3{\cdot}xH_2O$, $Fe(acac)_3$ and $(C_2H_5)_3NBH_3$ were taken in the molar ratios of Nd:Fe:B as 3.5:5.5:1 for the synthesis of $Nd_2Fe_{14}B$ nanoparticles. 2.1 mmol of $Nd(acac)_3{\cdot}xH_2O$ and 3.3 mmol of $Fe(acac)_3$ were dissolved in 120 mL of oleylamine under vigorous magnetic stirring condition. A 250 mL three-necked round bottom flask was used for the reactor connected to the standard Schlenk-line set-up. After stirring for 20 min, the solution was heated to 120 °C at a heating rate of 10 °C min^{-1} and maintained for 1 h under vacuum condition for the degassing process. Then, 0.6 mmol of $(C_2H_5)_3NBH_3$ was quickly injected to the solution and the solution was heated to 300 °C at a heating rate of 10 °C min^{-1} and maintained for 1 h under high purity Ar gas atmosphere. After 1 h maintained, the solution was cooled down to room temperature and precipitated in the mixed solvent (ethanol:hexane, v/v, 2:1). It was separated by centrifugation at 9000 rpm for 10 min and dried in vacuum chamber for 2 h.

Step 2: Reductive annealing process of as-synthesized Nd-Fe-B oxide powders

For the synthesis of $Nd_2Fe_{14}B$ magnetic nanoparticles by the reduction and diffusion process of as-synthesized Nd-Fe-B oxide powders, the powders were reduced under Ar+5% H_2 gas at 800 °C for 2 h at a heating rate of 5 °C min^{-1} to reduce iron oxides. After then, reduced powders were mixed with CaH_2 by hand grinding in a glove box. The weight ratio of the preliminary reduced metal oxide powders to CaH_2 was 1:1 and a compact pellet was prepared under the pressure of 300 kgf/cm^2 for 1 min. The pellet was put in an alumina crucible and transferred to a quartz tube furnace conditioned with flowing high purity Ar gas and annealed at 900 °C for 2 h at a heating rate of 5 °C min^{-1} for the reduction and diffusion process. The resultant products were completely washed with deionized water to remove impurities such as Ca and CaO. Finally, the products were washed with acetone to remove residual water and stored in 99.5% cyclohexane under high purity Ar gas to suppress the oxidation for the further characterization.

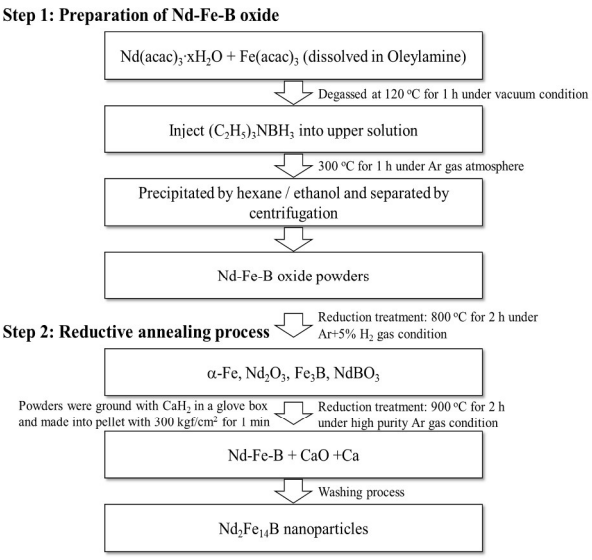

Figure 1. The flow diagram of the synthetic process of Nd2Fe14B magnetic nanoparticles.

ARTICLE View Article Online
DOI: 10.1039/C6NJ02456D Journal Name

Characterization

X-ray diffraction (XRD) patterns of the metal oxide powders and reduction products were obtained by using XRD (Rigaku Miniflex-desktop) with the Cu Kα radiation (λ=1.54056 Å) at 30 KV and 15 mA. The morphologies, EDS mapping and spectra of the products were measured with transmission electron microscope (TEM, JEOL. JEM-2100F, operated at 200 keV). The magnetic properties of final products were measured with a vibrating sample magnetometer (VSM, LakeShore 7400) at 300 K.

Results and Discussion

The synthesis of $Nd_2Fe_{14}B$ magnetic nanoparticles was carried out by two step process as shown in the flow diagram of Figure 1. The first step is the preparation of Nd-Fe-B oxide powders by using metal acetyl acetonate precursors and boron source. The second step is the reduction and diffusion process by using CaH_2 as a reducing agent. X-ray diffraction patterns of Nd-Fe-B oxide powders and $Nd_2Fe_{14}B$ hard phase magnet powders are shown in Figure S1 and Figure 2, respectively. Figure S1 shows that the main phase of the Nd-Fe-B oxide powders is Fe_3O_4 formed after the heat treatment during the first step. The existence of neodymium and boron elements was not detected in the XRD patterns because they are exist in amorphous phase, covering surrounding of the Fe_3O_4 nanoparticles (Figure S2). These Fe_3O_4 nanoparticles and amorphous phase composed of Nd and B elements were crystallized into Nd_2O_3, Fe_3B, $NdBO_3$ and α-Fe powders through the reductive annealing process of the second step synthesis conducting at 800 °C for 2 h under Ar+5% H_2 gas. The resultant XRD patterns are shown in Figure 2(a). The reduced metal oxide powders were mixed with CaH_2 granules with the different weight ratio of the preliminary produced metal oxides to CaH_2 as 1:0.4, 1:0.8, 1:1.0 and 1:1.2 (wt%) and the reduction/diffusion process was carried out after compaction

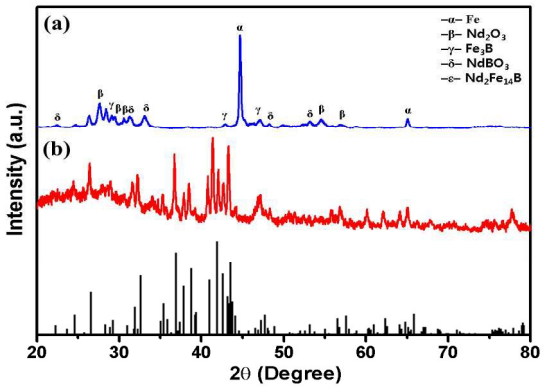

Figure 2. X-ray diffraction patterns of (a) Nd-Fe-B oxide powders after reduction at 800 °C for 2 h under Ar+5% H_2 gas and (b) $Nd_2Fe_{14}B$ powders after reduction and diffusion process at 900 °C for 2 h with CaH_2 under high purity Ar gas. Standard peaks positions for $Nd_2Fe_{14}B$ (JCPDS# 86-0273) are indicated at the bottom. Peaks corresponding to the α-Fe, Nd_2O_3, Fe_3B and $NdBO_3$ phases are marked by (α, JCPDS# 06-0696), (β, JCPDS# 28-0671), (γ, JCPDS# 39-1315) and (δ, JCPDS# 12-0756), respectively

process of the sample powders into pellet under the pressure of 300 kgf/cm^2 for 1 min. The as-prepared compact pellet was annealed at 900 °C for 2 h under high purity Ar gas atmosphere and the resultant products were shattered to be completely washed with deionized water to remove some impurities and un-reacted Ca and CaO. As a result, the metal oxide powders were completely reduced and transformed to the $Nd_2Fe_{14}B$ phase as shown in Figure 2(b). The detailed chemical reaction processes of the reactions are shown in the following equations.[22] (M stands for the metal or boron elements).

$$CaH_2 \rightarrow Ca + 2H \quad (1)$$

$$M_nO_m + mCa \rightarrow nM + mCaO \quad (2)$$

$$M + xH \rightarrow MH_x \quad (3)$$

$$2H \rightarrow H_2 \quad (4)$$

The dominant peaks of Figure 2(b) are pertaining to tetragonal structural $Nd_2Fe_{14}B$ phase (JCPDS# 86-0273), suggesting that the

Journal Name

View Article Online
DOI: 10.1039/C6NJ02456D

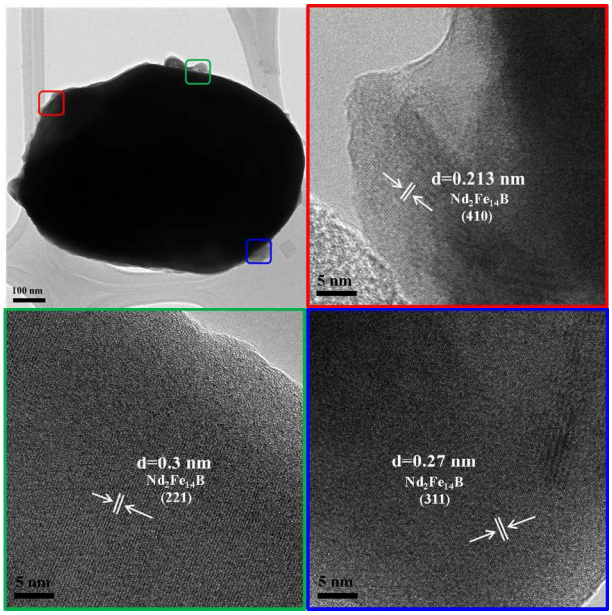

Figure 3. HRTEM images of $Nd_2Fe_{14}B$ magnetic nanoparticle produced by reductive annealing process of Nd-Fe-B oxide powders. The lattice spacing values of 0.213 nm, 0.3 nm and 0.27 nm are assigned to the (410), (221) and (311) planes of $Nd_2Fe_{14}B$, respectively.$Nd_2Fe_{14}B$ magnetic nanoparticles were produced after the reductive annealing process. HRTEM images also demonstrated the formation of $Nd_2Fe_{14}B$ magnetic nanoparticles (Figure 3). The HRTEM images of $Nd_2Fe_{14}B$ magnetic nanoparticles were taken from the edge parts of $Nd_2Fe_{14}B$ nanoparticles because of the agglomerated $Nd_2Fe_{14}B$ nanoparticles. The highlighted images as 'red', 'green' and 'blue' indicated that the nanoparticle is composed of nanoscale grains and they have various crystal lattice orientations. The lattice spacing values of 'red', 'green' and 'blue' were 0.213nm, 0.3 nm and 0.27nm matched with the (410), (221) and (311) planes of $Nd_2Fe_{14}B$ magnetic nanoparticles, respectively. The corresponding EDX elemental mapping and EDX spectrum is shown in Figure S3. In the EDX spectrum, the atomic ratio of Nd to Fe elements of the $Nd_2Fe_{14}B$ was 0.25 which is lower than the initial reactant molar ratio of Nd to Fe precursors because of the evaporation of Nd during reductive annealing process at 800 - 900 °C. On the other hand, the atomic ratio, 0.25, is higher than the standard atomic ratio of the

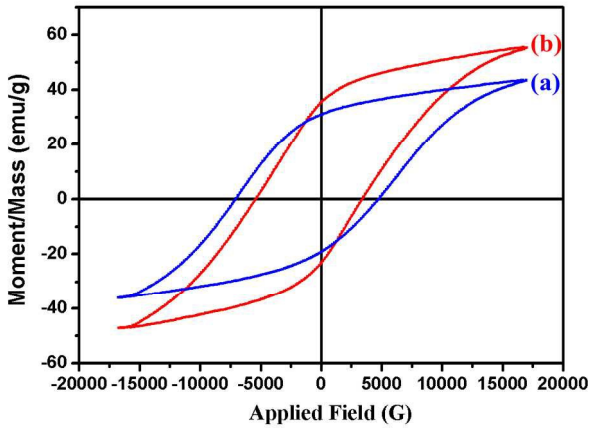

Figure 4. The magnetic hysteresis loops of Nd-Fe-B alloy after reductive annealing process measured with VSM measurement in the full magnetic field range at room temperature; (a) reduction products as synthesized and (b) final products after removal of Ca, CaO by washing process with DI water.

$Nd_2Fe_{14}B$ magnetic compound (Nd/Fe = 0.14) because some of the Nd elements are existing on void space among the surface of $Nd_2Fe_{14}B$ nanoparticles. The morphology of the produced $Nd_2Fe_{14}B$ particles (weight ratio: 1:1.0) is shown in Figure S4 (a). The size distribution is shown in Figure S4 (b). The shape and the size of the $Nd_2Fe_{14}B$ particles are not in regular and uniform because of the 900 ^oC reduction annealing. The size distribution was calculated from the size of 76 particles by the nano measure software. The average size is 980 nm.

The magnetic properties of $Nd_2Fe_{14}B$ magnetic nanoparticles were characterized by a magnetic hysteresis loop measured with VSM at 300 K as shown in Figure 4. The magnetic hysteresis curves were obtained with the reduced samples (a) as-synthesized and (b) after removal of Ca and CaO with water, respectively. From the magnetic hysteresis curves, it can be seen that the remanence value was increased after washing process because of the elimination of non-magnetic phases such as Ca and CaO. On the other hand, the coercivity value was decreased from 7066.6 G to 5407.9 G because of the partial decomposition of $Nd_2Fe_{14}B$ nanoparticles during

View Article Online
DOI: 10.1039/C6NJ02450D Journal Name

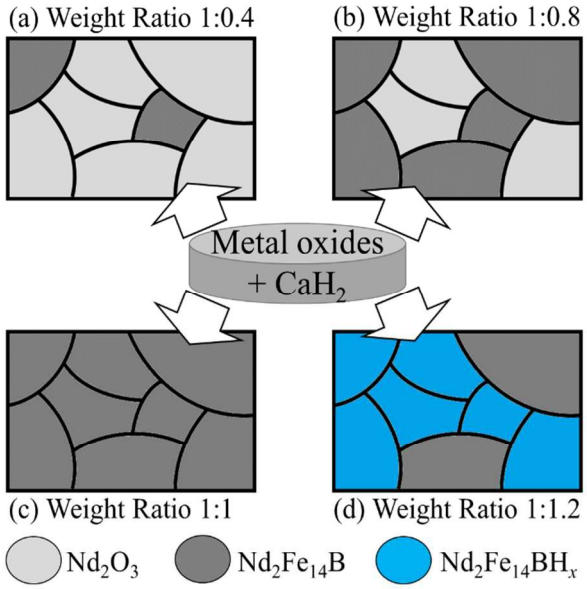

Figure 5. Schematic representation of the phases of Nd-Fe-B alloy produced by reductive annealing process of metal oxide powders with different weight ratio of the preliminary produced metal oxide powders to CaH_2; each phases belongs to the weight ratio of (a) 1:0.4, (b) 1:0.8, (c) 1:1.0 and (d) 1:1.2.

washing process. When the reduced samples were washed with DI water to remove the non-magnetic phases, an exothermic oxidation reaction might be occurred momently. It resulted in a partial decomposition of $Nd_2Fe_{14}B$ magnetic phase to soft magnetic phases of $Nd_2Fe_{17}B_x$ or α-Fe. Consequently, the magnetic properties of the final products were considerably reduced mostly because of the decomposition by the increase of reaction temperature.[23] The maximum energy products of the $Nd_2Fe_{14}B$ product (weight ratio: 1:1.0) before washing and after washing are determined as 1.7 MGOe and 1.9 MGOe, respectively, using a theoretical density of 7.5 g/cm^3, respectively.

In the reductive annealing process, the amount of CaH_2 as a reducing agent has a critical effect on the transformation of metal oxides to $Nd_2Fe_{14}B$ nanoparticles. The deficiency of CaH_2 results in remaining of Nd-Fe-B oxides powders. These remained Nd-Fe-B oxide powders decrease the magnetic properties of the final products. The excessive amount of CaH_2 can also decrease the magnetic

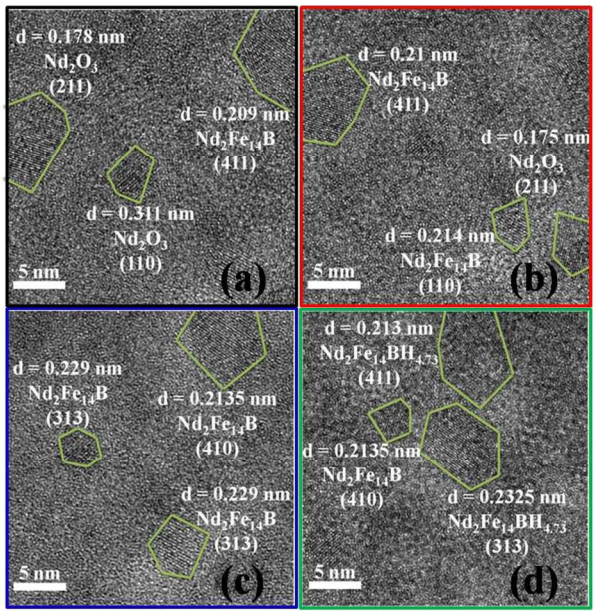

Figure 6. HRTEM images of Nd-Fe-B alloy produced by reductive annealing process of metal oxide powders with different weight ratio of CaH_2; each phases belong to the weight ratio of (a) 1:0.4, (b) 1:0.8, (c) 1:1.0 and (d) 1:1.2. In the HRTEM images of (a) and (b), the lattice spacing values matched with $Nd_2Fe_{14}B$ and Nd oxide phase due to the deficiency of CaH_2 for the reduction. The lattice spacing values of (c) exactly matched with $Nd_2Fe_{14}B$ and the lattice spacing values of (d) indicated that the excessive amount of CaH_2 influenced on the formation of $Nd_2Fe_{14}BH_{4.73}$.

properties of $Nd_2Fe_{14}B$ magnetic nanoparticles after reduction and diffusion process because of the vigorous evolution of H_2 gas during washing process with deionized water. In case of the excessive amount of CaH_2 condition, it was revealed that the formation of $Nd_2Fe_{14}BH_x$ due to evolution of H_2 gas decreases the magnetic properties of the $Nd_2Fe_{14}B$ compound.[24,25] The residual CaH_2 can react with deionized water and produce the $Ca(OH)_2$ and H_2 gas and the activated H_2 leads to the hydrogenation of the produced $Nd_2Fe_{14}B$ nanoparticles and decreases the magnetic properties dramatically as following chemical process in the equations.((5), (6))

Journal Name

View Article Online
DOI: 10.1039/C6NJ02456D

$$CaH_2 + 2H_2O \rightarrow Ca(OH)_2 + 2H_2 \quad (5)$$

$$Nd_2Fe_{14}B + 6H \rightarrow Nd_2Fe_{14}BH_x + \text{excess H } (x=1\text{-}5) \quad (6)$$

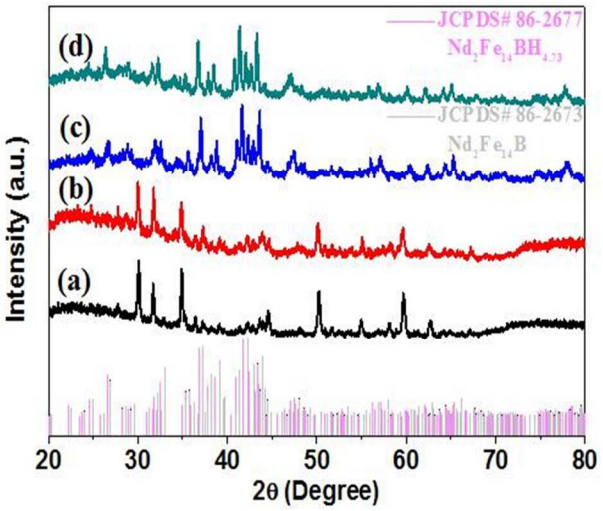

Figure 7. X-ray diffraction patterns of Nd-Fe-B alloy after reduction and diffusion process with the mixing weight ratio of CaH_2 to the reduced metal oxide powders; (a) 1:0.4, (b) 1:0.8, (c) 1:1.0 and (d) 1:1.2, respectively. The un-marked peaks maybe belonging to Nd based oxides phases.

effect of the amount of CaH_2 on reduction and diffusion process was comparatively investigated with the different mixing weight ratio (wt%) of the preliminary reduced metal oxide powders to CaH_2 and the products of the chemical reaction of each ratio were schematically shown in Figure 5. The resulted products were observed with HRTEM images and X-ray diffraction patterns as shown in Figure 6 and Figure 7. Before the compaction process, the weight ratio of the preliminary reduced metal oxide powders to CaH_2 was adjusted as 1:0.4, 1:0.8, 1:1.0 and 1:1.2, respectively.

Even though the pure $Nd_2Fe_{14}B$ nanoparticles were partially produced in the weight ratio of 1: 0:4, Nd based oxide phases were remained after reduction and diffusion process as observed from the HRTEM image in Figure 6(a) because of the deficiency of CaH_2 amount for reducing Nd based oxides to $Nd_2Fe_{14}B$ nanoparticles completely. Similarly, Nd based oxide phases were still remained in the weight ratio of 1:0.8 as observed in Fig. 6(b). On the other hand, with the weight ratio of 1:1.2, the excessive amount of CaH_2 had effect on the formation of $Nd_2Fe_{14}BH_{4.73}$ with pure $Nd_2Fe_{14}B$ nanoparticles as observed in the HRTEM image of Fig. 6(d) and detected slightly shifted peaks to lower 2θ angle as shown in XRD patterns of Fig. 7(d). It could be formed by the chemical reactions of

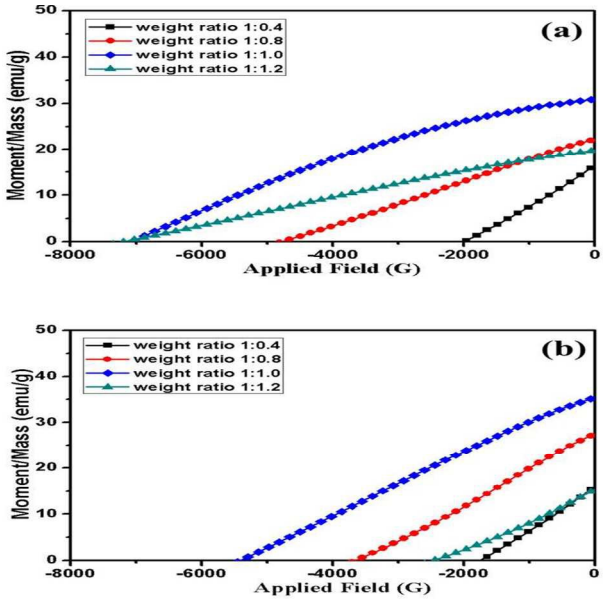

Figure 8. The magnetic hysteresis loops of Nd-Fe-B alloy with the different mixing weight ratio of the reduced metal oxide powders to CaH_2 (a) after reduction and diffusion process and (b) after washing process with DI water.

(5) and (6). As the amount of CaH_2 was added excessively above the weight ratio of 1:1.0, residual CaH_2 reacted with water and generated H_2 gas during washing process. The produced H_2 gas could be diffused into the lattice of $Nd_2Fe_{14}B$ magnetic nanoparticles interstitially and induced to form the $Nd_2Fe_{14}BHx$.

Consequently, excessive or deficient amount of CaH_2 can decrease the magnetic properties of $Nd_2Fe_{14}B$ nanoparticles by the different two mechanisms as observed from the magnetic hysteresis loops in Figure 8. From the difference of magnetic hysteresis loops between (a) and (b) of Figure 8, it is easy to find that the coercivity values were decreased dramatically in the ratio of 1.2, indicating that the most critical factor is the interstitially diffused H_2 gas and it decreases the magnetic properties of $Nd_2Fe_{14}B$ nanoparticles by partial hydrogenation into $Nd_2Fe_{14}BH_x$. In the weight ratio of 1:1.0, the metal oxides were completely reduced by CaH_2 and $Nd_2Fe_{14}B$ magnetic nanoparticles were successfully synthesized as observed in

View Article Online
DOI: 10.1039/C6NJ02456D Journal Name

Figure 6(c) and Figure 7(c), indicating that the optimum weight ratio of the reduced metal oxide powders to CaH_2 was very critical for the magnetic properties of the final products and determined to be 1:1:0.

Conclusions

Synthesis of $Nd_2Fe_{14}B$ magnetic nanoparticles was successfully carried out by chemical synthesis route followed by reduction and diffusion process. Comparing with the previously published articles, the NdFeB-O was synthesized in the organic environment, from the view of the TEM image in the Fig S2, the Fe-O was uniformly dispersed in the Nd-B-O matrix, besides the size of FeO is in nano-scale, so during the reduction and diffusion step, the Nd-B-O could be reduced and diffused into the reduced Fe nanoparticle. Then the nano-scale $Nd_2Fe_{14}B$ grains could be obtained. This chemical synthesis route is an easy method for the production of $Nd_2Fe_{14}B$ nanoparticles having a large coercivity value of 5407.9 G without consuming a large amount of energy. Through the first step, the Nd-Fe-B oxide powders were produced with metal acetyl acetonate precursors under heating operation relatively at low temperature and in a few hours. Because of the reducing ability of CaH_2, the Nd-Fe-B oxides were completely transformed to the $Nd_2Fe_{14}B$ nanoparticles at 800 - 900 °C. After washing process with water, we could obtain the pure $Nd_2Fe_{14}B$ nanoparticles. Moreover, it was revealed that the deficient amount of CaH_2 resulted in the low magnetic properties of final products because it was not enough to reduce metal oxides completely. On the contrary, the formation of $Nd_2Fe_{14}BH_x$ produced by excessive amount of CaH_2 resulted in the low magnetic properties. It was revealed that the amount of CaH_2 as a reducing agent is the critical factor of decreasing the magnetic properties of final products.

Notes and References

1 J. M. D. Coey, *Solid State Commun.,* 1997, **102**, 101-105.

2 M. Sagawa, S. Fujimura, N. Togawa, H. Yamamoto and Y. Matsuura, *J. Appl. Phys.,* 1984, **55**, 2083.

3 O. Gutfleisch, J. Phys. D: Appl. Phys., 2000, **33**, R157-R172.

4 N. Wang, B. J. Bowers and D. P. Arnold, *J. Appl. Phys.,* 2008, **103**, 07E109.

5 Y. Kanko, *IEEE Trans. Magn.,* 2000, **36**, 3275-3278.

6 H. Li, X. L, D. Guo, L. Lou, W. Li and X. Zhang, *Nano Lett.,* 2016, **16**, 5631-5638.

7 G. Bai, R. W. Gao, Y. Sun, G. B. Han and B. Wang, *J. Magn. Magn. Mater.,* 2007, **308**, 20-23.

8 F. J. Cadieu, *J. Appl. Phys.,* 1987, **61**, 4105-4110.

9 J. J. Croat, J. F. Herbst, R. W. Lee and F. E. Pinkerton, *J. Magn. Magn. Mater.,* 1999, **200**, 373.

10 E. F. Kneller and R. Hawig, *IEEE Trans. Magn.,* 1991, **27**, 3588–3600.

11 W. Liu, X. Z. Li, Y. C. Sui, J. Zhou, W. J. Ren, Z. D. Zhang and D. J. Sellmyer, *J. Appl. Phys.,* 2008, **103**, 07E130.

12 M. Nezakat, R. Gholamipour, A. Amadeh, A. Mohammadi and T. Ohkubo, *J. Magn. Magn. Mater.,* 2009, **321**, 3391–3395.

13 R. Zhang, Y. Liu, J. Li, S. Gao and M. Tu, *Mater. Charact.,* 2008, **59**, 642–646.

14 S. H. Sun, C. B. Murray, D. Weller, L. Folks and A. Moser, *Science.,* 2000, **287**, 1989–1992.

15 H. W. Zhang, S. Peng, C. B. Rong, J. P. Liu, Y. Zhang, M. J. Kramer and S. H. Sun, *J. Mater. Chem.,* 2011, **21**, 16873–16876.

16 Q. Zhang, Z. Jiang and B. Yan, Inorg. Chem. Front., 2014, 1, 384-388.

17 L. Q. Yu, Y. P. Zhang, Z. Yang, J. D. He, K. T. Dong and Y. Hou, *Nanoscale.,* 2016, **8**, 12879-12882.

18 L. Q. Yu, C. Yang and Y. L. Hou, *Nanoscale.,* 2014, 6, 10638-10642.

19 H. X. Ma, C. W. Kim, D. S. Kim, J. H. Jeong, I. H. Kim and Y. S. Kang, *Nanoscale.,* 2015, **7**, 8016.

20 C. W. Kim, Y. H. Kim, U. Pal and Y. S. Kang, *J. Mater. Chem. C.,* 2013, **1**, 275-281.

Journal Name

View Article Online
DOI: 10.1039/C6NJ02450B

21 V. Swaminathan, P. K. Deheri, S. D. Bhame and R. V. Ramanujan, *Nanoscale.,* 2013, **5**, 2718-2725.

22 P. K. Deheri, V. Swaminathan, S. D. Bhame, Z. W. Liu and R. V. Ramanujan, *Chem. Mater.,* 2010, **22**, 6509-6517.

23 T. S. Jang, D. H. Lee and S. Namkung, *Rev. Adv. Mater. Sci.,* 2011, **28**, 212-216.

24 D. Fruchart, L. Pontonnier, F. Vaillant, J. Bartolome, J. M. Fernandez, J. A. Puertolas, C. Rillo, J. R. Regnard, A. Yaouanc, R. Fruchart and P. L'Heritier, *IEEE Trans. Magn.,* 1988, **24**, 1641-1643.

25 B. Rupp, A. Resnik, D. Shaltiel and P. Rogi, *J. Mater. Sci.,* 1988, **23**, 2133-2141.

View Article Online
DOI: 10.1039/C6NJ02436J

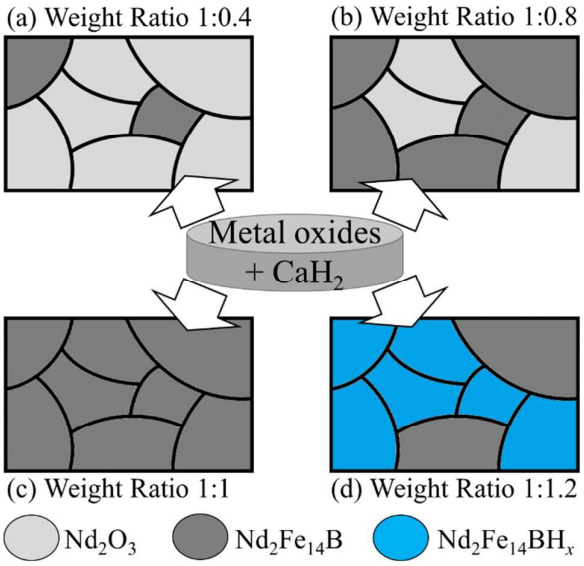

Short introduction: Schematic representation of the phases of Nd-Fe-B alloy produced by reductive annealing process of metal oxide powders with different weight ratio of the preliminary produced metal oxide powders to CaH_2 ; each phases belongs to the weight ratio of (a) 1:0.4, (b) 1:0.8, (c) 1:1.0 and (d) 1:1.2.